

Ambient Mass Spectrometry Imaging Metabolomics Method Provides Novel Insights into the Action Mechanism of Drug Candidates

Jingjing He,^{†,‡} Zhigang Luo,^{†,‡} Lan Huang,[§] Jiuming He,[†] Yi Chen,[‡] Xianfang Rong,[†] Shaobo Jia,[†] Fei Tang,[‡] Xiaohao Wang,[‡] Ruiping Zhang,[†] Jianjun Zhang,[†] Jiangong Shi,^{*,†} and Zeper Abliz^{*,†}

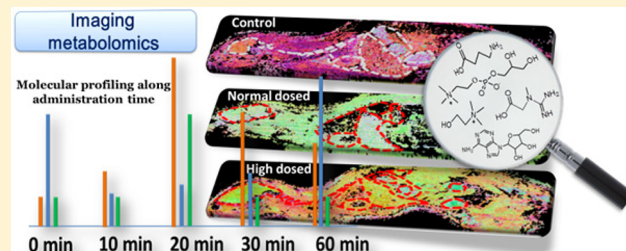
[†]State Key Laboratory of Bioactive Substance and Function of Natural Medicines, Institute of Materia Medica, Chinese Academy of Medical Sciences and Peking Union Medical College, Beijing 100050, People's Republic of China

[‡]State Key Laboratory of Precision Measurement Technology and Instruments, Department of Precision Instruments and Mechanology, Tsinghua University, Beijing 100084, People's Republic of China

[§]Institute of Laboratory Animal Science, Chinese Academy of Medical Sciences and Peking Union Medical College, Beijing 100021, People's Republic of China

S Supporting Information

ABSTRACT: Elucidation of the mechanism of action for drug candidates is fundamental to drug development, and it is strongly facilitated by metabolomics. Herein, we developed an imaging metabolomics method based on air-flow-assisted desorption electrospray ionization mass spectrometry imaging (AFADESI-MSI) under ambient conditions. This method was subsequently applied to simultaneously profile a novel anti-insomnia drug candidate, *N*⁶-(4-hydroxybenzyl)-adenosine (NHBA), and various endogenous metabolites in rat whole-body tissue sections after the administration of NHBA. The principal component analysis (PCA) represented by an intuitive color-coding scheme based on hyperspectral imaging revealed *in situ* molecular profiling alterations in response to stimulation of NHBA, which are in a very low intensity and hidden in massive interferential peaks. We found that the abundance of six endogenous metabolites changed after drug administration. The spatiotemporal distribution indicated that five altered molecules—including neurotransmitter γ -aminobutyric acid, neurotransmitter precursors choline and glycerophosphocholine, energy metabolism-related molecules adenosine (an endogenous sleep factor), and creatine—are closely associated with insomnia or other neurological disorders. These findings not only provide insights into a deep understanding on the mechanism of action of NHBA, but also demonstrate that the AFADESI-MSI-based imaging metabolomics is a powerful technique to investigate the molecular mechanism of drug action, especially for drug candidates with multitarget or undefined target in the preclinical study stage.



Discovering functional endogenous metabolites with extremely low content and their minor alterations is very important for understanding the complex biochemical processes, and it is beneficial to the success of the lengthy, high-risk, and costly drug development process.¹ It requires not only the elucidation of the molecular entities but also their spatial distribution within the organism. Current analytical methods, including mass spectrometry imaging (MSI) and metabolomics, despite having fundamental development, still face challenges for elucidating comprehensive and multiple molecular spatiotemporal dynamics involving stimulating biological process.

Thus, far, MSI² has allowed hundreds of known and unknown molecules to be simultaneously located and identified together with histological features of biological samples, avoiding tedious preparation of labeled analytes prior to analysis. Several well-developed MSI-based technologies are currently in use.^{3–9} Among these, secondary ionization mass spectrometry (SIMS)-MSI,⁴ matrix-assisted laser desorption ionization (MALDI)-

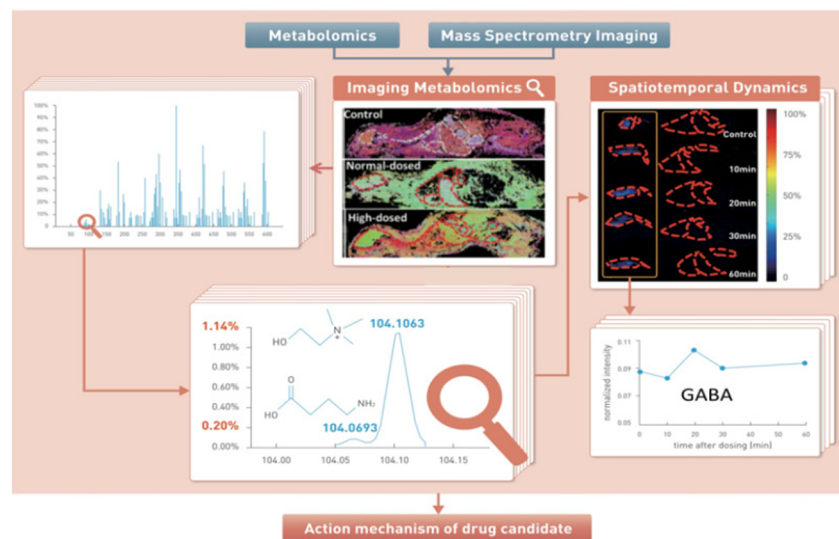
MSI,^{5,6} and desorption electrospray ionization (DESI)-MSI under ambient conditions^{7–9} are the three frontrunners. With regard to drug and drug metabolite profiling,^{10,11} several studies have utilized MSI methods to differentially measure drug and metabolite ion signatures in rat whole-body tissue sections^{12–15} and organ compartments.^{9,16} However, there is still room for improvement of MSI to better visualize trace drugs at therapeutic levels, to assess the distribution alteration of endogenous metabolites after drug administration,^{17,18} and to compare distinct ion signals within and between different organs or animals. Despite these drawbacks, MSI has recently expanded its applications for endogenous metabolites to provide new insights into pharmacological and toxicological mechanisms, facilitating clinical diagnosis of complex diseases.^{19–24}

Received: February 18, 2015

Accepted: April 15, 2015

Published: April 15, 2015



Scheme 1. Strategy of Imaging Metabolomics

Metabolomics has the potential to enhance our understanding on the molecular basis for mechanisms of drug action and predict variation in drug response.²⁵ The application of metabolomics for the study of global metabolite profiles under divergent drug administration conditions to predict drug effects and variation in drug response is creating "pharmacometabolomics".^{22,25,26} MSI (including MALDI-MSI, DESI-MSI, etc.) is currently the best choice for the performance of imaging metabolomics, because of its capacity to provide both molecular and spatial information simultaneously. Air-flow-assisted desorption electrospray ionization (AFADESI)-MSI under ambient conditions is a new technique that has been recently developed by our group.^{27,28} It is competent in large objects analysis because the high flow-rate extracting air flow was introduced to improve ion collection and remote transport efficiency and to promote charged droplets desolvation. AFADESI-MSI can easily map drugs and drug metabolites in large whole-body tissue sections with high sensitivity and specificity. Therefore, AFADESI-MSI becomes a strong complement in imaging metabolomics study, especially with regard to whole-body rat tissue sections with a large size. Taking advantages of AFADESI-MSI, herein, we present the first example of MSI-based imaging metabolomics approach to investigate the molecular mechanisms of drug candidate. First, an anti-insomnia drug candidate, *N*⁶-(4-hydroxybenzyl)-adenosine (NHBA), and various endogenous metabolites in whole-body tissue sections were simultaneously detected using the AFADESI-MSI technique. Subsequent hyperspectral MSI analysis revealed *in situ* abundance changes of the endogenous metabolites following drug stimulation. After structure identification and biological elucidation of the found metabolites with significant changes, six endogenous metabolites highly associated with sedative and hypnotic effects of NHBA were successfully mined and spatiotemporally characterized in the rat, providing new insights into understanding on the action mechanism of the drug candidate. The strategy of imaging metabolomics is shown in Scheme 1.

■ EXPERIMENTAL SECTION

Material and MSI Instruments. Formic acid was purchased from Sigma-Aldrich (St. Louis, MO). HPLC-grade methanol and acetonitrile were purchased from Merck (Muskegon, MI).

Pure water was obtained from a local market (Wahaha, Hangzhou, China). NHBA was obtained from Professor Jiangong Shi (Institute of Materia Medica, Chinese Academy of Medical Sciences (CAMS), Beijing, China). NHBA was prepared as an aqueous stock solution of 4 mg/mL in 0.9% NaCl plus Tween 80 (1:100 v:v). Male Wistar rats were purchased from the Institute of Laboratory Animal Science at CAMS.

MSI experiments in full-scan mode were performed by using a quadrupole time-of-flight mass spectrometer (QSTAR Elite, Applied Biosystems, Foster, CA/MDS Sciex, Concord, ON, Canada), and MSI experiments in MRM scan mode were performed by using a QTRAP 5500 mass spectrometer (AB SCIEX, Framingham, MA). Both spectrometers were equipped with custom-made air-flow-assisted desorption electrospray ionization (AFADESI) ion sources.

Preparation of Whole-Body Tissue Sections. The animal study was approved by the Animal Care and Welfare Committee of the Institute of Materia Medica, CAMS and Peking Union Medical College (Beijing, China) (Approval Nos. 0215506 and 0260214).

Adult male Wistar rats weighing ~140–160 g were used in the experiment. After fasting for 24 h, control rats were intraperitoneally injected with 40 mg/kg saline plus Tween 80 (1:100 v:v), whereas high-dosed rats were intraperitoneally injected with 300 mg/kg NHBA in 8 mg/mL saline plus Tween 80 (1:100 v:v), and normal-dosed rats were intraperitoneally injected with 40 mg/kg NHBA in 4 mg/mL saline plus Tween 80 (1:100 v:v). The rats were euthanized under CO₂ gas at 20 min after drug/vehicle administration, snap-frozen in a liquid nitrogen bath, embedded/blocked in 3.5% aqueous carboxymethyl cellulose, and frozen at -80 °C until sectioning. Snap freezing was done to quench any biological reactions in the body, given that the molecular turnover of bioactive endogenous metabolites is rapid. Sagittal whole-body cryosections (40 μm thick) were then prepared using a Leica CM3600 cryomacrotome (Leica Microsystems Ltd., Wetzlar, Germany). All sections were stored at -80 °C until use and dried in a vacuum desiccator for 1 h prior to analysis to minimize post-mortem changes.²⁹

Optical images of whole-body tissue sections were acquired with a Microtek scanner (MRS-2400A48U, Shanghai Microtek Technology Ltd., Shanghai, China). Because molecular profiles

vary from section to section within a three-dimensional (3D) organism, only tissue sections from the same layer are comparable between animals. To obtain tissue sections from the same layer in different animals, a layer located at a depth of 3.84 mm below the layer with the first exposure of brain tissue was selected for sectioning and imaging. Most of the major organs were exposed in the selected layer.

MSI Analysis. All MSI experiments were performed with a custom-made AFAEI ion source in DESI mode. For the MS parameters in full-scan mode, nebulizer gas (denoted as GS1), drying gas (denoted as GS2), and curtain gas were set at 80, 0, and 10, respectively. The source temperature was set at “heat off”. The declustering potential was 68, and the focusing potential was 250. The transport tube voltage was set at 1200 V, which was the same as the voltage applied to the curtain plate. The data were collected by using the “enhance all” full-scan function, and data were acquired over a specified mass range (m/z 100–600) by setting the focusing rod offset at 20. The MS parameters in MRM scan mode were similar to those used in our previous work.²⁸

MRM analysis was applied for the detection of NHBA (m/z 374.2 → 242.0) and the six endogenous metabolites (m/z 104.1 → 69.0, m/z 104.1 → 60.0, m/z 118.1 → 72.0, m/z 132.1 → 90.0, m/z 268.0 → 136.0, and m/z 258.1 → 104.0). The dwell time was set at 200 ms. These transition settings were established according to the MS spectra and product ion spectra of NHBA and the metabolites (see the Supporting Information).

Data Processing. Raw spectra were stored in .wiff format and changed to mzML files with the msconvert function in ProteoWizard 3.0.4445 software (available at <http://proteowizard.sourceforge.net/downloads.shtml>). Next, the mzML files for the control and NHBA-treated rats, as well as NHBA-dosed rats at different time points, were integrated into one imzML³⁰ file per condition by using the imzMLconverter (<http://www.maldi-msi.org>). Images were created by using Data Cube Explorer software (FOM Institute AMOLF, The Netherlands, available from www.maldi-msi.org) with a bin size of 0.1 (sum of all signals in the m/z window), and the entire data set was saved as one .dat file. The data for each m/z value were exported and saved as a .csv file (mass range, 100–600; 5000 m/z values in total) by using the C++ program (FOM Institute AMOLF). A homemade script was used to import the .csv files into Matlab R2012b (MathWorks, Natick, MA), resulting in a matrix with rows representing the (x,y) position of the mass spectrum, and columns representing the m/z variables. In this way, the three-dimensional imaging data array was reduced to a two-dimensional matrix, thereby retaining the (x,y) location of each spectrum for use in image reconstruction.

Clean data matrices were obtained after performing the following sequential data preprocessing steps to compare peak intensities across different pixels: peak selection, pixel selection, normalization, logarithmic scaling, and mean-centering. This data processing methodology used the presence of typical chemical background interferences in ambient ionization and m/z values with clear outlines of whole-body rat sections as references to select biologically informative m/z peaks. For pixel selection, pixels that clearly did not arise from sample regions were discarded based on the ratio of the total ion current (TIC) value of the informative peaks (after peak selection) to the TIC value of all 5000 variables. The remaining data matrix was then normalized to the TIC value of the biologically informative peaks. Logarithmic scaling was performed in subsequent modeling steps to increase the importance of lower intensity but still structurally informative variables, followed by mean-

centering of the data, which subtracts the average intensity for each m/z variable.³¹ Lastly, the PCA results were represented by an intuitive color-coding scheme based on hyperspectral imaging methods.^{32,33}

RESULTS AND DISCUSSION

Drug Imaging. NHBA is a novel neuroprotective compound isolated at trace levels from the rhizome of *Gastrodia elata* Blume (Orchidaceae family), which is an indispensable Chinese herbal medicine (Tianma in Chinese), exhibiting activity at a dose of 0.2 mg/kg in mice following intraperitoneal injection. Our previous studies confirmed that NHBA is an anti-insomnia compound that acts within the brains of mice through simultaneous activation of adenosine A₁ and A_{2A} receptors.³⁴ However, NHBA is still under preliminary research and, therefore, detailed evaluations of the compound are urgently required in relation to its metabolism, pharmacokinetics, and mechanism of action.

To understand the pharmacokinetic features of NHBA, NHBA pharmacokinetics was first studied by using quantitative rapid resolution liquid chromatography/tandem mass spectrometry (RRLC-MS/MS) method in multiple reaction monitoring (MRM) in rat brainstems. The drug was metabolized and excreted within 240 min (Figure 1a). However, NHBA content was quite low in the brainstem, even at peak concentration (~70 pg/mg). This result suggests that only a small amount of the compound penetrated the blood brain barrier (BBB) and distributed into the target brain tissue.

NHBA was then spatially mapped by AFADESI-MSI in rat whole-body tissue sections, which were prepared at the time

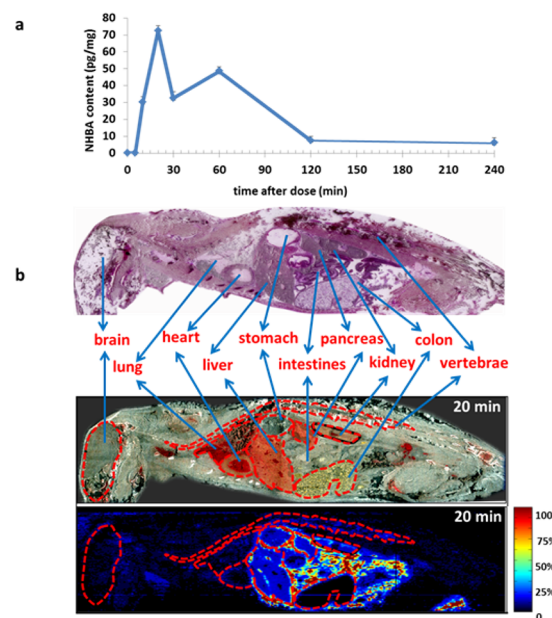


Figure 1. NHBA content in the rat brainstem and whole-body distribution. (a) NHBA content in the brainstem of rats euthanized at various time points after dosing, as measured by quantitative LC-MS/MS in MRM mode (see the Supporting Information for details). (b) Whole-body distribution of NHBA (40 mg/kg via intraperitoneal injection, followed by euthanasia 20 min later) acquired by AFADESI-MSI (MRM, m/z 374.2 → 242.0). Organ regions are outlined. Spatial resolution = 300 μ m × 500 μ m. ((Top panel) HE-stained, whole-body rat tissue section at 20 min after NHBA administration; (middle panel) optical image of rat tissue section; and (bottom panel) MSI image of rat tissue section.

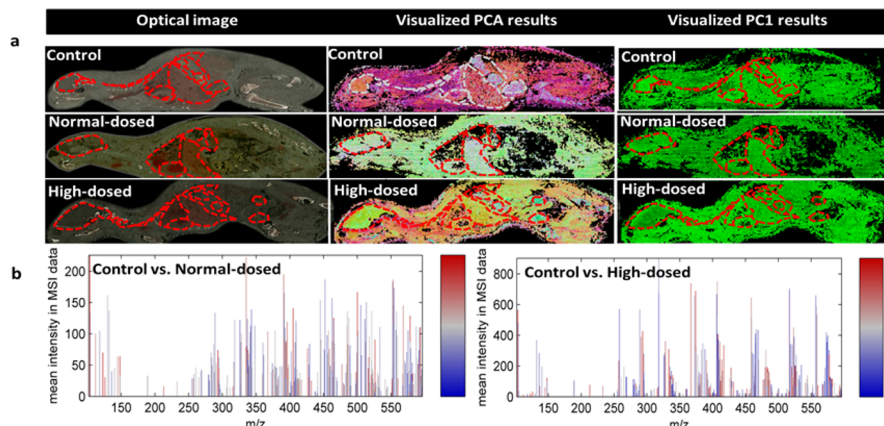


Figure 2. Visualization of PCA/PC1 results of MSI data and molecular profiles with m/z bin size = 0.1. (a) Optical images and visualized PCA/PC1 results of MSI data acquired by AFAADESI-MSI in full-scan mode, comparing control rats with normal-dosed rats (40 mg/kg NHBA via intraperitoneal injection, followed by euthanasia 20 min later) and high-dosed rats (300 mg/kg NHBA, followed by euthanasia 20 min later). For the visualized PCA results, the PCA score value for each pixel on each of the first three components determined the intensity for the red, green, and blue (RGB) channels, respectively. For the visualized PC1 results, the score value of each pixel on the first PC (PC1) in the PCA model determined the intensity of the green channel. (b) Loading for PC1 in the PCA model yielded bright red peaks with large positive weights on PC1, and bright blue peaks with a negative weight on PC1. The height of the peaks corresponds to the average signal intensity of the normalized data (before log-transformation and mean-centering) (see ref 32).

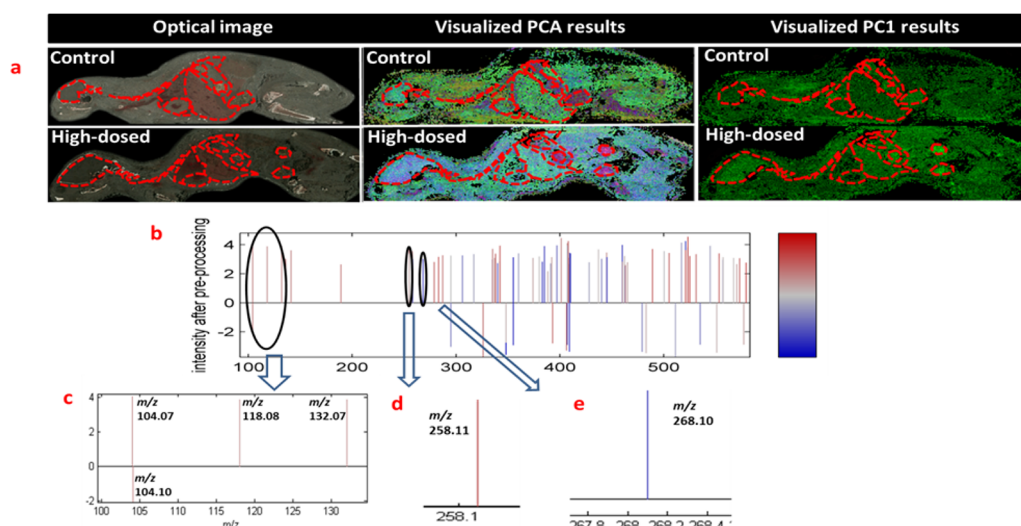


Figure 3. Visualization of PCA results of significantly discriminated peaks and molecular profiles with m/z bin size = 0.01. (a) Optical images and visualized PCA/PC1 results of MSI data acquired by AFAADESI-MSI in positive full-scan mode, comparing control rats with high-dosed rats at 20 min after dosing. PCA and PC1 results were visualized as described in the figure legend. (b) Loading for PC1 in the PCA model yielded bright red peaks with large positive weights on PC1, and bright blue peaks with a negative weight on PC1. The height of the peak corresponds to the signal intensity after normalization, log-transformation, and mean-centering. (c–e) Expanded views of significantly discriminated m/z peaks (m/z 104.07, m/z 104.10, m/z 118.08, m/z 132.07, m/z 258.11, and m/z 268.10) (see the Supporting Information).

when the peak NHBA concentration was observed (20 min after dosing). This image (Figure 1b) demonstrates that NHBA was mainly accumulated in intestines. By contrast, only a small amount of compound distributed into the vertebrae, and very little distributed into the brain.

Moreover, NHBA images in rat head sections at 10, 20, and 30 min after the administration of 40 mg/kg NHBA; from the upper, middle, and lower portions of one rat head; and from rats at 20 min after administration of NHBA at concentrations of 40, 150, and 300 mg/kg all demonstrate that very low content of NHBA distribute in the targeted organs of anti-insomnia (see the Supporting Information). Taking the obvious sedative and hypnotic effects of NHBA into consideration, we hypothesized

that these small amounts of NHBA in targeted organs are able to bring significant changes to the body.

Mining and Characterization of NHBA-Responsive Endogenous Metabolites via Visualized Principal Component Analysis (PCA). To understand how the trace NHBA in the target organ had the sedative and hypnotic effect, we sought to characterize the specific responding molecules of drug action via AFAADESI-MSI-based imaging metabolomics approach. In this investigation, a whole-body tissue section preparation protocol (see the Experimental Section, specifically the subsection entitled “Preparation of Whole-Body Tissue Sections”) was optimized and strictly followed to ensure that all revealed metabolites were biologically relevant, and that the

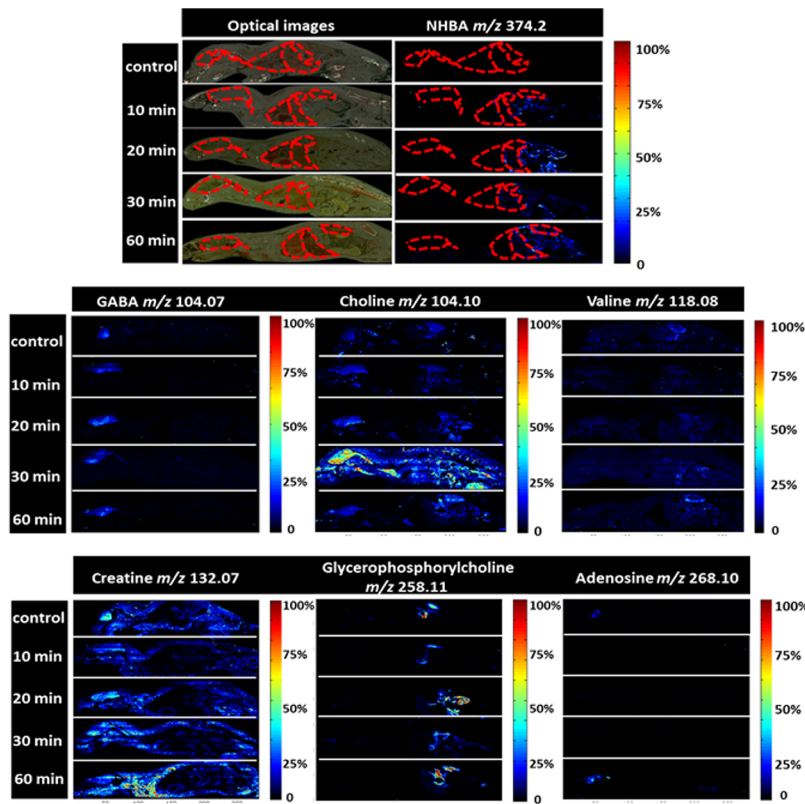


Figure 4. Optical images of whole-body tissue sections at different time points after administration of NHBA, and spatiotemporal visualization of NHBA and six endogenous metabolites in rat whole-body tissue sections. Rats were given NHBA (40 mg/kg via intraperitoneal injection) and euthanized 10 min, 20 min, 30 min, or 1 h later. MSI data were acquired by AFADESI-MSI (MRM, NHBA: m/z 374.2 → 242.0; GABA: m/z 104.1 → 69.0; choline: m/z 104.1 → 60.0; valine: m/z 118.1 → 72.0; creatine: m/z 132.1 → 90.0; glycerophosphocholine: m/z 258.1 → 104.0; adenosine: m/z 268.0 → 136.0). Spatial resolution = 300 μ m × 500 μ m.

observed molecular changes and abundances were comparable among different tissue sections.

In situ molecular profiles of whole-body sections of control, normal-dosed (40 mg/kg NHBA), and high-dosed (300 mg/kg NHBA) rats were acquired by AFADESI-MSI in full-scan mode with a mass range of m/z 100–600. Necessary and appropriate data preprocessing steps were implemented to compare peak intensities across different pixels³¹ (see the Supporting Information). A data matrix with 322 biological informative peaks \times 39 699 pixels was under a PCA analysis with each pixel measured via MSI to yield score values reflecting molecular contents. The score value of each pixel on the first three PCs in the PCA model (PC1, PC2, and PC3) determined the intensity of the red, green, and blue channels, respectively, in the image. Thus, pixels with similar mass spectra had similar image colors.³²

The PCA images (Figure 2a, middle column) of whole-body sections from control (top), normal-dosed (middle), and high-dosed (bottom) rats yielded consistent molecular profiles in each of the outlined organs in the optical images (Figure 2a, left column), signifying that the molecular profiles were similar for each organ throughout the whole-body tissue sections. By contrast, the color differences between the PCA images of control, normal-dosed, and high-dosed whole-body sections exhibited varying molecular profiles after NHBA administration. The PC 1 images (Figure 2a, right column, displayed in green for visual clarity) showed molecular profile variations in the brain, liver, and intestines of control versus NHBA-treated rats. Furthermore, the intense blue loading color in Figure 2b is indicative of a higher prevalence of corresponding m/z values in

the brain, liver, and intestines of NHBA-treated rats vs control rats, while the opposite situation prevails for the red loading color.

To identify the endogenous metabolites most significantly altered by NHBA administration and to decrease interference from the mixed spectra of overlapping metabolites, 98 distinctive m/z values at a bin width of 0.01 (see the Supporting Information) were selected to perform visualized PCA (Figure 3). The comparison of the control and high-dosed whole-body sections revealed that most of the 98 selected peaks represented significant increases or decreases. By searching the public databases (METLIN (<http://metlin.scripps.edu/>) and HMDB (<http://hmdb.ca/>)) in reference to accurate mass and isotope patterns, as well as filtering metabolites related with sedative and hypnotic effect, we focused on the red peaks with m/z 104.07, 104.10, 118.08, 132.07, and 258.11 (protonated ions) increasing in the brain, liver, and intestines after NHBA administration, and the blue peak with m/z 268.10 (protonated ions) decreasing in the corresponding organs (see Figure 3b).

Next, we compared the MS/MS spectra with those of commercially available, authentic standards (see the Supporting Information). As a result, endogenous metabolites possessing these six m/z data were identified as γ -aminobutyric acid (GABA, m/z 104.07), choline (m/z 104.10), valine (m/z 118.08), creatine (m/z 132.07), glycerophosphocholine (m/z 258.11), and adenosine (m/z 268.10) (see Figures 3c–e). Fortunately, these endogenous metabolites, with the exception of the indispensable amino acid valine, are all well-defined molecules that are closely associated with the treatment of insomnia and

other neurological disorders. Therefore, the AFADESI-MSI-based metabolomics approach employed herein successfully uncovered probable mechanistic pathways of NHBA action at the small molecular level in rats.

Spatiotemporal and Dynamic Analysis of NHBA and Altered Small Molecules. Next, NHBA and altered small molecules were targeted and analyzed in MRM mode with high sensitivity and specificity at various time points after drug administration. This was done to acquire spatiotemporal information regarding the drug candidate and the altered molecules, to further understand their relationship with sedative/hypnotic effects. We found that molecular images detected in MRM mode were consistent with those detected in full-scan mode (see the Supporting Information), enhancing our confidence about the molecular assignment of peaks with an intensity too low for the procurement of MS/MS fragments.

Because whole-body MSI utilizes intact animals that have not been processed to any great extent, thus reducing intersample experimental variability,³⁵ only one animal was analyzed for each time point. Figure 4 presents optical images (left column) and AFADESI-MSI images (right column) of NHBA and the six endogenous metabolites in rat whole-body tissue sections at 10, 20, 30, and 60 min after NHBA administration (40 mg/kg via intraperitoneal injection), representing their spatiotemporal distributions. As expected, NHBA was not observed in the whole-body section of the control rat, whereas in drug-treated rats, NHBA was mainly accumulated in the intestines, with maximum intensity being observed 20 min after dosing.

The γ -aminobutyric acid (GABA), in the brain, increased with the maximum at 20 min, consistent with that of the NHBA distribution, and returned to the normal level 10 min later. Choline drastically increased in the whole body, with the maximum content being observed 30 min after dosing (Figure 5), while glycerophosphorylcholine increased in the kidney and the intestines, with the maximum content at 20 min. In addition, the levels of creatine continuously increased in the brain and muscle-rich regions. On the other hand, adenosine levels dramatically decreased, with a minimum attained at 10–30 min, and then increased to levels much higher than normal at 60 min after NHBA administration (Figure 5). Finally, valine levels steadily increased in the kidney and the intestines (Figure 4).

The novel anti-insomnia drug candidate, NHBA, shows good therapeutic potential in the treatment of insomnia and other neurodegenerative conditions, including Huntington's disease, Alzheimer's disease, and Parkinson's disease.³⁶ The consistency between the findings attained herein by quantitative RRLC-MS/MS MRM and AFADESI-MSI indicates that NHBA actions are induced by trace amounts of drug distributed within the target organ, the brain. We anticipated that NHBA administration would provoke substantial molecular responses in the host and, indeed, this hypothesis was confirmed by the identification and characterization of six endogenous metabolites, GABA, choline, glycerophosphocholine, adenosine, creatine, and valine.

GABA is one of the most important inhibitory neurotransmitters in the brain, and increased levels of GABA reduce anxiety and favor sleep.^{37,38} Moreover, changes in GABA content and GABAergic neurotransmission are also associated with neurodegeneration in Huntington's disease, Alzheimer's disease, and Parkinson's disease.³⁶ Choline and glycerophosphocholine are precursors of the neurotransmitter acetylcholine, which promotes sleep and participates in memory, muscle control, etc.³⁹ Adenosine is an energy metabolite with the function of regulating the sleep–wake cycle.^{40–43} Creatine also functions in

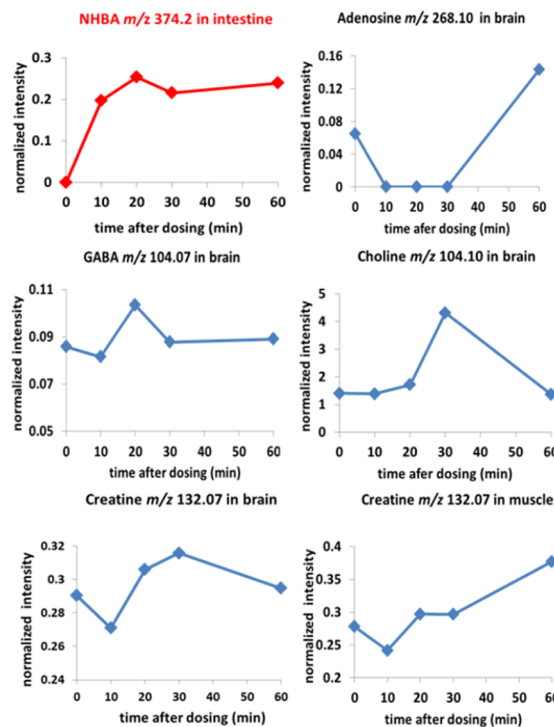


Figure 5. Abundance trends of NHBA and endogenous metabolites. The mean intensity values after normalization were calculated within a certain region and plotted against time after dosing.

energy metabolism by increasing the formation of adenosine triphosphate (ATP) to supply energy to every cell in the body and helps to overcome brain fatigue and improve mood following sleep deprivation.⁴⁴

The functions of GABA, choline, glycerophosphocholine, adenosine, and creatine are consistent with the sedative and hypnotic effects of NHBA. Therefore, alteration of the levels of these molecules in response to NHBA clearly reveals a pharmacological network of multiple mechanistic pathways of drug action, corresponding to the GABAergic, cholinergic, adenosinergic, and metabolic energy systems and their physiological relationships. The six endogenous metabolites may be the “mechanistic small molecules” of drug action. This study confirmed that NHBA has a multiple-target mechanism of action, and can be potentially developed as a drug candidate for the treatment of insomnia and related neurological disorders. Nonetheless, far more information is still hidden in the enormous MSI database and further mining for endogenous metabolites is expected in the future.

Moreover, our successful visualization of NHBA distribution and elucidation of mechanistic molecules of drug action now firmly establishes the highly anticipated potential of AFADeSI-MSI^{27,28} and other MSI methods in drug discovery and development, especially in uncovering the complicated mechanistic networks and pathways of drug action at the small molecular level.

CONCLUSIONS

In conclusion, the imaging metabolomics based on air-flow-assisted desorption electrospray ionization mass spectrometry imaging (AFADESI-MSI) is able to sensitively and reliably discover *in situ* low-level abundance changes of six mechanistic small molecules responding to *N*⁶-(4-hydroxybenzyl)-adenosine (NHBA), action from a huge spectral dataset and massive

interferential peaks. These altered endogenous metabolites provided significant insights into therapeutic responses associated with drug action.

The present findings indicate that imaging metabolomics can accelerate pharmaceutical development in searching for drug action mechanisms, pathways, and targets, as well as possible side effects and toxicities at the whole-body level. Although the current imaging metabolomics method still faces some challenges, such as ion suppression from different organs/regions may affect the intensity comparability, variant may come from the different ionization efficiency of various analytes and the ionized metabolites may be limited due to the MS ionization ability. With the development of MSI techniques (e.g., quantitative imaging, etc.) and robust multivariate statistical analysis (e.g., effective normalization), we anticipate that this approach will be especially useful during the early preclinical stages of drug development, permitting the identification of drug candidates with superior metabolic properties and mechanisms for a focused and detailed investigation, even in the fields of single cell metabolomics,⁴⁵ *in situ* biomarker discovery, and early disease diagnosis.⁴⁶

ASSOCIATED CONTENT

Supporting Information

Materials, detailed experimental procedures and supplementary figures are in the Supporting Information. This material is available free of charge via the Internet at <http://pubs.acs.org/>.

AUTHOR INFORMATION

Corresponding Authors

*E-mail: zeper@imm.ac.cn (Z. Abliz).

*E-mail: shijg@imm.ac.cn (J. Shi).

Author Contributions

[†]These authors contributed equally.

Author Contributions

Z.A. designed the research and supervised all of the research work; Z.A., J.G.S., J.J.H., and Z.G.L. planned the experiments; J.J.H. and Z.G.L. performed the AFADESI-MSI analysis and pharmacokinetic analysis of NHBA; J.G.S. provided NHBA, the investigated object; L.H., X.F.R., and S.B.J. prepared the tested animals and tissue sections; J.M.H., Y.C., F.T., and X.H.W. built the AFADESI-MSI system; J.J.H. analyzed data; J.J.H. and Z.G.L. wrote the manuscript; Z.A., J.G.S., and J.M.H. revised the manuscript; Z.A., J.G.S., J.J.H., Z.G.L., J.M.H., J.J.Z., and R.P.Z. discussed pharmacological mechanisms and biological information on drug action.

Notes

The authors declare no competing financial interest.

ACKNOWLEDGMENTS

The authors thank the National Scientific and Technological Major Project for New Drugs (2012ZX09301002-001-006 and 2012ZX09103101-001), the National Instrumentation Program (2011YQ170067) and PCSIRT (No. IRT1007) for financial support.

REFERENCES

- (1) Willmann, J. K.; van Bruggen, N.; Dinkelborg, L. M.; Gambhir, S. S. *Nat. Rev. Drug Discovery* **2008**, *7*, 591–607.
- (2) Caprioli, R. M.; Farmer, T. B.; Gile, J. *Anal. Chem.* **1997**, *69*, 4751–4760.

- (3) Liu, Y.; Ma, X.; Lin, Z.; He, M.; Han, G.; Yang, C.; Xing, Z.; Zhang, S.; Zhang, X. *Angew. Chem.* **2010**, *122*, 4537–4539.
- (4) Monroe, E. B.; Jurchen, J. C.; Lee, J.; Rubakhin, S. S.; Sweedler, J. V. *J. Am. Chem. Soc.* **2005**, *127*, 12152–12153.
- (5) Seeley, E. H.; Caprioli, R. M. *Proc. Natl. Acad. Sci. U.S.A.* **2008**, *105*, 18126–18131.
- (6) Xiaodong, W.; Jun, H.; Juncong, Y.; Jingxi, P.; Christoph, H. B. *Chem. Sci.* **2015**, *6*, 10.
- (7) Takats, Z.; Wiseman, J. M.; Gologan, B.; Cooks, R. G. *Science* **2004**, *306*, 471–473.
- (8) Wu, C.; Dill, A. L.; Eberlin, L. S.; Cooks, R. G.; Ifa, D. R. *Mass Spectrom. Rev.* **2013**, *32*, 218–243.
- (9) Wiseman, J. M.; Ifa, D. R.; Zhu, Y.; Kissinger, C. B.; Manicke, N. E.; Kissinger, P. T.; Cooks, R. G. *Proc. Natl. Acad. Sci. U.S.A.* **2008**, *105*, 18120–18125.
- (10) Sun, N.; Walch, A. *Histochem. Cell Biol.* **2013**, *140*, 93–104.
- (11) Nimesh, S.; Mohottalage, S.; Vincent, R.; Kumarathasan, P. *Int. J. Mol. Sci.* **2013**, *14*, 11277–11301.
- (12) Khatib-Shahidi, S.; Andersson, M.; Herman, J. L.; Gillespie, T. A.; Caprioli, R. M. *Anal. Chem.* **2006**, *78*, 6448–6456.
- (13) Stoeckli, M.; Staab, D.; Schweitzer, A. *Int. J. Mass Spectrom.* **2007**, *260*, 195–202.
- (14) Trim, P. J.; Henson, C. M.; Avery, J. L.; McEwen, A.; Snel, M. F.; Claude, E.; Marshall, P. S.; West, A.; Princivalle, A. P.; Clench, M. R. *Anal. Chem.* **2008**, *80*, 8628–8634.
- (15) Kertesz, V.; Van Berkem, G. J.; Vavrek, M.; Koeplinger, K. A.; Schneider, B. B.; Covey, T. R. *Anal. Chem.* **2008**, *80*, 5168–5177.
- (16) Cornett, D. S.; Frappier, S. L.; Caprioli, R. M. *Anal. Chem.* **2008**, *80*, 5648–5653.
- (17) Miura, D.; Fujimura, Y.; Wariishi, H. *J. Proteomics* **2012**, *75*, 5052–5060.
- (18) Römpf, A.; Spengler, B. *Histochem. Cell Biol.* **2013**, *139*, 759–783.
- (19) Lietz, C. B.; Gemperline, E.; Li, L. *Adv. Drug Delivery Rev.* **2013**, *65*, 1074–1085.
- (20) Miura, D.; Fujimura, Y.; Yamato, M.; Hyodo, F.; Utsumi, H.; Tachibana, H.; Wariishi, H. *Anal. Chem.* **2010**, *82*, 9789–9796.
- (21) Shrivastava, K.; Hayasaka, T.; Sugiura, Y.; Setou, M. *Anal. Chem.* **2011**, *83*, 7283–7289.
- (22) Sugiura, Y.; Setou, M. *J. Neuroimmune Pharmacol.* **2010**, *5*, 31–43.
- (23) Eberlin, L. S.; Norton, I.; Orringer, D.; Dunn, I. F.; Liu, X.; Ide, J. L.; Jarmusch, A. K.; Ligon, K. L.; Jolesz, F. A.; Golby, A. J. *Proc. Natl. Acad. Sci. U.S.A.* **2013**, *110*, 1611–1616.
- (24) Eberlin, L. S.; Mulcahy, J. V.; Tzabazis, A.; Zhang, J.; Liu, H.; Logan, M. M.; Roberts, H. J.; Lee, G. K.; Yeomans, D. C.; Du Bois, J.; Zare, R. N. *J. Am. Chem. Soc.* **2014**, *136*, 6401–6405.
- (25) Kaddurah-Daouk, R.; Weinshilboum, R. M. *Clin. Pharmacol. Ther.* **2014**, *95*, 154–167.
- (26) Nicholson, J. K.; Connelly, J.; Lindon, J. C.; Holmes, E. *Nat. Rev. Drug Discovery* **2002**, *1*, 153–161.
- (27) He, J.; Tang, F.; Luo, Z.; Chen, Y.; Xu, J.; Zhang, R.; Wang, X.; Abliz, Z. *Rapid Commun. Mass Spectrom.* **2011**, *25*, 843–850.
- (28) Luo, Z.; He, J.; Chen, Y.; He, J.; Gong, T.; Tang, F.; Wang, X.; Zhang, R.; Huang, L.; Zhang, L. *Anal. Chem.* **2013**, *85*, 2977–2982.
- (29) Sugiura, Y.; Zaima, N.; Setou, M.; Ito, S.; Yao, I. *Anal. Bioanal. Chem.* **2012**, *403*, 1851–1861.
- (30) Schramm, T.; Hester, A.; Klinkert, I.; Both, J.-P.; Heeren, R.; Brunelle, A.; Laprévote, O.; Desbenoit, N.; Robbe, M.-F.; Stoeckli, M. *J. Proteomics* **2012**, *75*, 5106–5110.
- (31) Fonville, J. M.; Carter, C.; Cloarec, O.; Nicholson, J. K.; Lindon, J. C.; Bunch, J.; Holmes, E. *Anal. Chem.* **2012**, *84*, 1310–1319.
- (32) Fonville, J. M.; Carter, C. L.; Pizarro, L.; Steven, R. T.; Palmer, A. D.; Griffiths, R. L.; Lalor, P. F.; Lindon, J. C.; Nicholson, J. K.; Holmes, E. *Anal. Chem.* **2013**, *85*, 1415–1423.
- (33) Pirro, V.; Eberlin, L. S.; Oliveri, P.; Cooks, R. G. *Analyst* **2012**, *137*, 2374–2380.
- (34) Zhang, Y.; Li, M.; Kang, R.-X.; Shi, J.-G.; Liu, G.-T.; Zhang, J.-J. *Pharmacol. Biochem. Behav.* **2012**, *102*, 450–457.
- (35) Solon, E. G. *Chem. Res. Toxicol.* **2012**, *25*, 543–555.

- (36) Lei, Y.; Wang, L.; Cheng, M.; Xiao, H. *Biomed. Chromatogr.* **2011**, *25*, 344–352.
- (37) Blankenberg, F. G. *J. Cell. Biochem.* **2003**, *90*, 443–453.
- (38) Gottesmann, C. *Neuroscience* **2002**, *111*, 231–239.
- (39) McCarley, R. W. *Sleep Med.* **2007**, *8*, 302–330.
- (40) Scammell, T. E.; Estabrooke, I. V.; McCarthy, M. T.; Chemelli, R. M.; Yanagisawa, M.; Miller, M. S.; Saper, C. B. *J. Neurosci.* **2000**, *20*, 8620–8628.
- (41) Strecker, R. E.; Moraarty, S.; Thakkar, M. M.; Porkka-Heiskanen, T.; Basheer, R.; Dauphin, L. J.; Rainnie, D. G.; Portas, C. M.; Greene, R. W.; McCarley, R. W. *Behav. Brain Res.* **2000**, *115*, 183–204.
- (42) Kong, J.; Shepel, P. N.; Holden, C. P.; Mackiewicz, M.; Pack, A. I.; Geiger, J. D. *J. Neurosci.* **2002**, *22*, 5581–5587.
- (43) Basheer, R.; Strecker, R. E.; Thakkar, M. M.; McCarley, R. W. *Prog. Neurobiol.* **2004**, *73*, 379–396.
- (44) McMorris, T.; Harris, R. C.; Swain, J.; Corbett, J.; Collard, K.; Dyson, R. J.; Dye, L.; Hodgson, C.; Draper, N. *Psychopharmacology* **2006**, *185*, 93–103.
- (45) Zenobi, R. *Science* **2013**, *342*, 1243259.
- (46) Perkel, J. M. *Science*, DOI: 10.1126/science.opms.p1300076.